

# The Spectroscopic Studies on the Aggregation Behavior of Cyanine Dyes

Hyungsik Min, Jeunghee Park\*, Jongwan Yu<sup>†</sup>, and Dongho Kim<sup>‡</sup>

*Department of Chemistry, Korea University, 208 Seochngdong, Jochiwon, Chungnam 339-700, Korea*

*<sup>‡</sup>Spectroscopy Laboratory, Korean Research Institute of Standards and Science,  
Taedok Science Town, Taejon 305-500, Korea*

*Received February 6, 1998*

Aggregations of 1,1'-diethyl-2,2'-carbocyanine iodide (DCI) and 1,1'-diethyl-2,2'-dicarbocyanine iodide (DDI) in aqueous solution have been investigated by the steady-state absorption spectroscopy. The equilibrium constants for dimerization of DCI and DDI are found to be  $(9.8 \pm 0.5) \times 10^4$  and  $(1.6 \pm 0.5) \times 10^5 \text{ M}^{-1}$ , respectively, at 293 K. The enthalpy changes for the dimerization of DCI and DDI are  $-6.7 \pm 0.7$  and  $-7.7 \pm 0.8 \text{ kcal/mol}$ , respectively. The results show that the dispersion force plays an important role in the aggregation of DCI and DDI in aqueous solution. The absorption bandwidth of DCI/ethanol system has been measured as a function of temperature, providing the evidence for no strong interaction between DCI and solvent molecules. The participation of hydrophobic force in driving the aggregation is suggested. For the first time, DCI in aqueous solution is found to form a new aggregate which has both J- and H- bands.

## Introduction

The cyanine dyes are a remarkable class of strong light absorbers, widely used in sensitizing the silver halide microcrystals in photographic films. The formation of aggregated dye molecules in the liquid state is important in photographic technology, tunable lasers, and photomedicines.<sup>1</sup> Since the formation of aggregates modifies the absorption spectrum and photophysical properties of a dye, it affects the ability of dye to emit at a certain wavelength and to act as a photosensitizer. The strength of aggregation between two or more dye molecules usually depends on the structure of the dye, the type of solvent, the temperature, and the presence of electrolytes. For the mechanism of aggregation, several driving forces such as additive van der Waals force, intermolecular hydrogen bonding, hydrogen bonding with the solvent, and coordination with metal ions, have been suggested.<sup>2-4</sup> Each of these driving forces can be only applied to the corresponding specific dye/solvent system. As an instance, in the dimerization of fluorescein and its halogenated derivatives, the nature of driving force changes with the extent of halogenation and the solvent.<sup>3</sup> For the symmetric thiocyanines in aqueous solution, it is suggested that the dispersion force is the main driving force in dimerization.<sup>5</sup>

In this paper, we have investigated the nature of driving force for the aggregation of symmetric carbocyanine dyes such as 1,1'-diethyl-2,2'-carbocyanine iodide (DCI) and 1,1'-diethyl-2,2'-dicarbocyanine iodide (DDI) in aqueous solution. Analysis of the changes in the steady-state absorption spectrum with dye concentration and temperature was adopted to obtain the equilibrium constant as well as thermodynamic data for the aggregation process. The molecular exciton theory simply offers a theoretical description of the aggregation by considering the interactions between the tran-

sition dipole moments of the molecule.<sup>6</sup> In this work, this exciton model is employed to explain the spectral shift of the cyanine aggregates and predict the geometries of the aggregates.

## Experimental

DCI (Aldrich, 98%) and DDI (Exciton, 98%) were used as received without further purification. All solvents used in this experiment are the spectrophotometric grades. Absorption spectra were collected by a multichannel spectrophotometer coupled with the optical fiber, using a 100 W Xenon arc lamp as a light source. The concentration ranges of DCI and DDI solutions were  $1.5 \times 10^{-6}$ – $7.0 \times 10^{-5} \text{ M}$  and  $6.0 \times 10^{-7}$ – $2.4 \times 10^{-5} \text{ M}$ , respectively.

Temperature dependent spectra were collected by using a cell (3.4 mm path length) which was vacuum-tightly sealed by a Viton O-ring. The cell was mounted on the cold finger (Janis C-210) of a cryostat (Leybold-Heraeus) whose temperature was controlled within 0.2 K by a autotuning temperature controller (Lakeshore 330). The temperature range used in aqueous solutions is 275–330 K. For 1:1 water:ethylene glycol (EG) solution, the temperature range is 250–300 K. The fluorescence spectrum was measured by an Aminco SLM-8000 spectrofluorometer.

## Results and Discussions

Figure 1(A) shows the absorption spectrum as a function of DCI concentration in aqueous solution, at 293 K. Over the range of DCI concentrations, the increase of aggregation formation is shown by the growth of a new absorption band at  $18,400 \text{ cm}^{-1}$ , which can be attributed to the dimer. As the dye ion is further increased, a new additional band at  $19,200 \text{ cm}^{-1}$  appears. The band at  $19,200 \text{ cm}^{-1}$  must be attributed to the higher aggregate (trimer or tetramer) than the dimer. The same procedure was done for DDI in aqueous solution. The absorption peaks of DDI monomer, dimer, and trimer or tetramer were found to be at  $14,300 \text{ cm}^{-1}$ ,<sup>7</sup>

\*Author to whom correspondence should be addressed.

<sup>†</sup>Present address: Department of Chemistry, Won Kwang University, 370-949, Korea

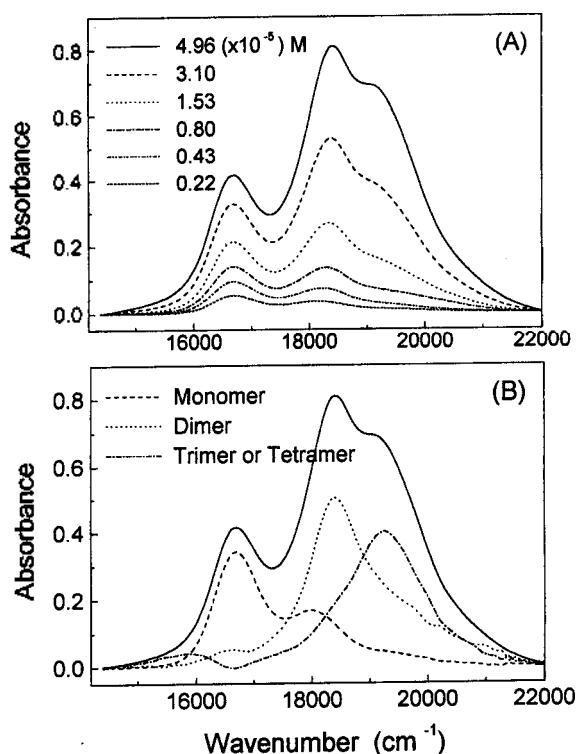


**Figure 1.** (A) The absorption spectrum of aqueous DCI as a function of concentration at 293 K. The 2-mm length cell is used. (B) The absorption spectrum of aqueous  $5.0 \times 10^{-5}$  M DCI, resolved into the monomer, dimer, and trimer or tetramer bands.

$16,200 \text{ cm}^{-1}$ ,<sup>8</sup> and  $17,100 \text{ cm}^{-1}$ , respectively.

According to the 1-dimensional exciton model,<sup>6</sup> the absorption peak shift of the aggregate relative to the monomer is given by

$$\Delta\nu = \frac{2}{h} \frac{N-1}{N} \frac{\langle m^2 \rangle}{r^2} (1 - \cos^2 \theta), \quad (1)$$

where  $N$  is the degree of polymerization of the aggregate,  $\Delta\nu$  is the spectral shift from monomer peak,  $h$  is the Planck's constant,  $r$  is the separation of molecular centers, and  $\theta$  is the tilt angle between the line of centers and molecular long axes. The  $\langle m^2 \rangle$  is the transition dipole moment of monomer,  $9.185 \times 10^{-39} \int_{\lambda_1}^{\lambda_2} \epsilon(d\lambda/\lambda)$ , where  $\epsilon$  is the molar extinction coefficient in  $\text{M}^{-1}\text{cm}^{-1}$ ,  $\lambda$  is the wavelength, and  $\lambda_1$  and  $\lambda_2$  are the limits of well-defined absorption band. By performing the integral on monomer spectrum, we obtained the values of  $13,800 \text{ M}^{-1}\text{cm}^{-1}$  and  $20,700 \text{ M}^{-1}\text{cm}^{-1}$ , respectively, for  $\int_{\lambda_1}^{\lambda_2} \epsilon(d\lambda/\lambda)$  of DCI and DDI, which agree with the values in ethanol.<sup>7</sup>

From Eq. (1), the spectral shift from the monomer peak is used to calculate the intermolecular separations in dimer. Assuming the angle  $\theta$  as  $90^\circ$ , the distances are calculated to be  $7.2 \text{ \AA}$  and  $7.9 \text{ \AA}$ , respectively, for DCI and DDI, which are longer than the typical intermolecular distance  $\sim 3 \text{ \AA}$  observed in the solid phase of other photographic sensitizing dyes.<sup>9</sup> It is noteworthy that the 1-dimensional exciton model which ignores the molecular structure and is originally derived for explaining the aggregation behavior in solid phase may not provide correct intermolecular distances in aqueous

solution. If the molecules aggregate with the same angle and distance, the peaks at  $19,200 \text{ cm}^{-1}$  in the DCI spectrum and  $17,100 \text{ cm}^{-1}$  in the DDI spectrum can be each attributed to their tetramer, not trimer. This possibility will be discussed later.

Figure 1(B) shows the resolved absorption bands of the monomer and the aggregates for  $5.0 \times 10^{-5}$  M DCI spectrum. The absorption band of DCI monomer can be obtained at low concentration limit  $10^{-7}$  M, where the band shape becomes independent on the concentration. From the measured spectrum at the concentration range,  $1.5 \times 10^{-6} \sim 8.0 \times 10^{-6}$  M, showing only monomer and dimer peaks, some multiple of the monomer spectrum was subtracted to obtain the dimer spectrum. By same procedure, the absorption band of higher aggregate has been obtained from the spectra of more concentrated solutions ( $10^{-5}$  M  $\sim 7 \times 10^{-5}$  M), as shown in Figure 1(B).

The absorption coefficient of the dimer was determined by the following procedure. The equilibrium for the dimer formation can be represented by  $2 \text{ M} \leftrightarrow \text{D}$ , where M and D represent the monomer and dimer, respectively. We introduced the parameters  $C_0$  as the concentration of dye,  $\epsilon_m$  and  $\epsilon_d$  as the integrated absorption coefficients of the monomer and the dimer, respectively, and  $A_{tot}$  as the total integrated absorbance. And  $A_M$  is the integrated absorbance of monomer at a given concentration where only monomer exists,  $\alpha$  is the degree of dimerization,  $\gamma$  is the absorption coefficient ratio of dimer to monomer, and  $l$  is the cell length. At equilibrium, the concentrations of monomer and dimer are  $(1-\alpha)C_0$  and  $(\alpha/2)C_0$ , respectively.

$$A_{tot} = \epsilon_m l (1-\alpha)C_0 + \epsilon_d l (\alpha/2)C_0$$

Since  $\epsilon_d = \gamma \epsilon_m$  and  $\epsilon_m l C_0 = A_M$ ,

$$\begin{aligned} A_{tot} &= \epsilon_m l (1-\alpha)C_0 + \gamma \epsilon_m l (\alpha/2)C_0 \\ A_{tot}/A_M &= 1 - \alpha + (\alpha/2)\gamma \\ A_{tot}/A_M &= 1 - (1-\gamma/2)\alpha \end{aligned} \quad (2)$$

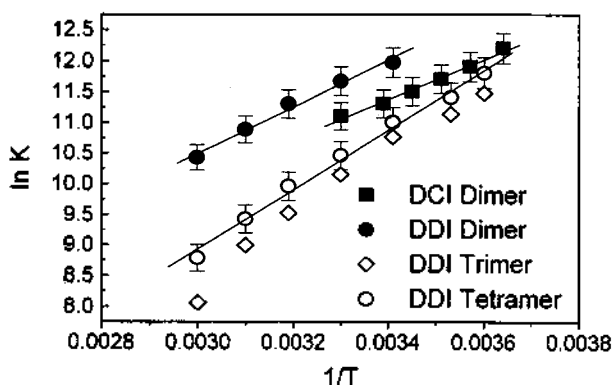
From the plot of  $A_{tot}/A_M$  vs.  $\alpha$ , the absorption coefficient ratio of dimer to monomer ( $\gamma$ ) can be obtained. At the concentration of  $3.7 \times 10^{-5}$  M where the formation of higher aggregates is negligible, the ethanol was added into the aqueous solution up to 10% by mole fraction. At 10% ethanol solution, no dimerization is observed so that  $A_M$  can be obtained. The spectrum as a function of ethanol mole fraction was resolved into monomer and dimer bands,  $A_{tot}/A_M$  is plotted as a function of  $\alpha$ , which gives  $\gamma = 1.6 \pm 0.05$  from a linear slope. The result that the ratio doesn't follow the additive rule indicates a strong interaction between the monomers. For DDI, with the same procedure, the absorption coefficient ratio was measured to be the same as that of DCI.

Knowing the absorption coefficients of the monomer and the dimer, one can obtain the concentrations of each species from the spectra measured at various temperatures and concentrations. For the dimer formation of DCI and DDI, the equilibrium constants at 293 K are  $(9.8 \pm 0.5) \times 10^4 \text{ M}^{-1}$  and  $(1.6 \pm 0.5) \times 10^5 \text{ M}^{-1}$ , respectively.

Thermodynamic data are obtained from the equilibrium constants at various temperatures. Table 1 lists the  $\Delta H^\circ$  and  $\Delta S^\circ$  values for the dimerization, obtained from the van't Hoff equation,  $\partial \ln K / \partial (1/T) = -\Delta H^\circ / R$ . Figure 2 shows the

**Table 1.** Equilibrium constants and thermodynamic parameters for the aggregation of DCI and DDI

Dye aggregate	Solvent	K (293 K)	$\Delta H^\circ$ (kcal/mol)	$\Delta S^\circ$ (cal/mol K)
DCI	dimer	$(9.8 \pm 0.5) \times 10^4$	$-6.7 \pm 0.7$	$-0.1 \pm 0.1$
	tetramer	$(5.2 \pm 0.3) \times 10^4$	-	-
DDI	dimer	$(1.6 \pm 0.5) \times 10^5$	$-7.7 \pm 0.8$	$-2.5 \pm 0.5$
	tetramer	$(6.0 \pm 0.5) \times 10^4$	$-9.8 \pm 1.0$	$-12 \pm 1$
DCI	water:EG 1:1 mixture	$(1.5 \pm 0.1) \times 10^3$	$-14 \pm 1$	$-33 \pm 2$

**Figure 2.** Van't Hoff plots for aggregation of DCI and DDI in aqueous solution. Assuming the higher aggregate of DDI as the trimer and the tetramer (see text), the data points are shown as the symbols  $\diamond$  and  $\circ$ , respectively. The fitted line for the tetramer data points ( $\circ$ ) is drawn to obtain the thermodynamic data.

van't Hoff plot for the dimerization of DCI and DDI, giving  $\Delta H^\circ = -6.7 \pm 0.7$  kcal/mol for DCI and  $\Delta H^\circ = -7.7 \pm 0.8$  kcal/mol for DDI. The equilibrium constant of dimerization (293 K) in the 1:1 mole ratio mixture of water and ethylene glycol is measured to be  $(1.5 \pm 0.1) \times 10^3$ . The value of  $\Delta H^\circ$  is  $-14 \pm 1$  kcal/mol.

When the  $19,200 \text{ cm}^{-1}$  band is assumed to be the trimer band, we found that the equilibrium constant for its formation increases with the concentration. However, if this band is the tetramer band, the equilibrium constant for the tetramer formation gives a reliably constant value throughout the whole concentration range. Assuming this band as the tetramer band, the absorption spectra at the  $8 \times 10^{-6}$ – $7 \times 10^{-5} \text{ M}$  at 293 K were analyzed to obtain the equilibrium constant for the tetramer formation as  $(5.2 \pm 0.3) \times 10^4 \text{ M}^{-1}$ . The absorption coefficient of the DCI tetramer is calculated to be 2.8 times of that of monomer.

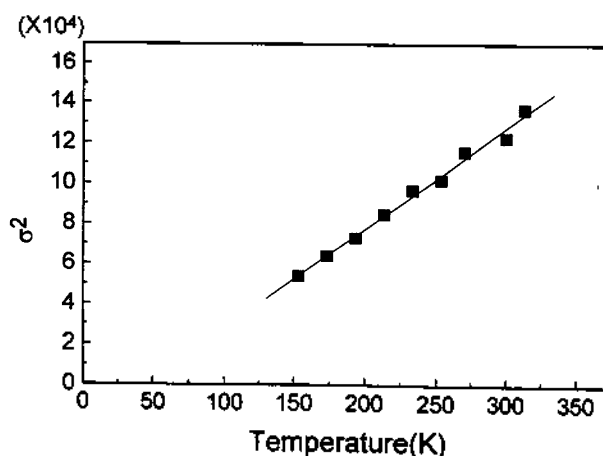
In the case DDI, when the band at  $17,100 \text{ cm}^{-1}$  is assigned to the trimer, its formation constant also increases with concentration. However, assuming that this band is the tetramer band, its formation constant is obtained as a constant values and its van't Hoff plot is better linearly fitted to give more accurate  $\Delta H^\circ$  value, as shown in Figure 2. Figure 2 also shows the van't Hoff plot for the possible trimerization. For the tetramer formation, the values of  $\Delta H^\circ$  and  $\Delta S^\circ$  are obtained as  $-9.8 \pm 1.0$  kcal/mol and  $-12 \pm 1$  cal/mol K, respectively. The equilibrium constant at 293 K is  $(6.0 \pm 0.5) \times 10^4 \text{ M}^{-1}$ .

The  $-\Delta H^\circ$  value increases with the polymethine chain

length and the number of monomer in the aggregate, indicating that the dispersion force plays an important role in the aggregation of DCI and DDI dyes in aqueous solution. West and Pearce reported that the equilibrium constants for the dimer formation of 3,3'-diethylthiacarbocyanine iodide and 3,3'-diethylthiadibenzocarbocyanine iodide are  $2.9 \times 10^4 \text{ M}^{-1}$  and  $6.7 \times 10^4 \text{ M}^{-1}$ , respectively, at 295 K.<sup>5</sup> Graves and Rose reported its value as  $\sim 1 \times 10^3 \text{ M}^{-1}$  by using a Fourier transform proton magnetic resonance technique.<sup>10</sup> Kaiser and his coworkers reported the concentration dependence of dimerization constant of pseudoisocyanine chloride, and its value is in the order of  $10^3 \text{ M}^{-1}$  at 293 K.<sup>11</sup> Our results are consistent with those reported results; due to dispersion force the increase in the size of heterocyclic ring and the polymethine chain length of cyanine dye induces the equilibrium constant increase.

In EG/water solution,  $-\Delta H^\circ$  and  $-\Delta S^\circ$  values of DCI dimerization are much larger than those of water solution, and the formation constant become less. It is noticed that almost zero entropy change in DCI/water dimerization results in large formation constant. It is well known that hydrophobic interactions are entropy-driven.<sup>3</sup> Therefore, one possible explanation is that in aqueous solution the hydrophobic force is dominant to drive the dimerization, while in mixed EG/water solution the hydrophobic force is diminished so that the dimer formation is less favorable. The dimerization in mixed polar solvent must be investigated more carefully in future.

The hydrophobic interaction in DCI aqueous solution was checked by measuring the solute-solvent interaction in the DCI/ethanol system, which solvates DCI more strongly than water. Absorption spectrum of DCI in ethanol solution was measured as a function of temperature, showing that as the temperature was decreased from 315 K to 150 K, a significant line narrowing was observed without any appearance of new absorption bands. Figure 3 shows that the square of absorption line width  $\sigma^2$  as a function of temperature. The absorption line is usually broadened by two processes; the phonon relaxation and the structural relaxation. As the phase is changed from liquid to glass, the

**Figure 3.** The square of the full width at half maximum,  $\sigma^2$ , of the absorption band of DCI in ethanol as a function of temperature ( $\blacksquare$ ). The solid line is a linearly fitted line to the data points.

structural broadening is expected to remain almost the same, while the phonon width is decreased. The structural broadening is directly related to the statistical distribution of solvated molecules, while the phonon broadening is due to the very fast lattice-like vibrational motion which is intrinsic in all condensed phases. Yu and Berg expanded the theory of phonon modulated interactions with electronic transition in solid,<sup>12</sup> to the phonon-like broadening in the glassy and liquid solution systems.<sup>13</sup> They showed that the phonon width ( $\sigma_F^2$ ) can be given by Eq. 3 as follows:

$$\sigma_F^2 = \frac{h\nu}{2} \sum_F \coth\left(\frac{h\nu}{2kT}\right), \quad (3)$$

where  $\Sigma_F$  represents the Stokes shift due to the phonon broadening, and  $\nu$  represents the average value of the lattice phonon frequencies in the amorphous phase. At high temperature limit,  $\sigma^2$  is approximately to be linearly dependent on the temperature,

$$\sigma_F = kT \Sigma_F. \quad (4)$$

It is found that the square of line width of DCI in ethanol as a function temperature fits to straight line and the  $\sigma^2$  is extrapolated to zero as the temperature is decreased to 0 K, as shown in Figure 3. This result indicates that the phonon broadening contributes dominantly to the absorption width of DCI/ethanol solution. It is reasonable that the phonon broadening due to intrinsic vibrational process should be more dominant for the aqueous system where the solubility of cyanine is much smaller than the ethanol system. This interpretation is consistent with the fact that there is no strong interaction such as hydrogen bonding between DCI monomer and water. The water molecules around DCI molecule actually become more ordered during the solvation. If two DCI molecules cluster together, the disruptive effect on the solvent network will be less than the dispersive interaction of two separated DCI. This hydrophobic interaction could be important in the dimerization of DCI. We suggest that the aggregation of DCI can be driven by the hydrophobic force and the DCI molecules hold together exclusively by dispersion force.

The formation of higher order molecular aggregates can be observed in various environment such as the addition of salt or colloidal particles or the freezing process.<sup>14</sup> In this work, the spectrum showing two unreported bands is obtained by adding 0.2 M NaCl into  $10^{-3}$  M DCI aqueous solution. The spectrum of aqueous DCI  $10^{-3}$  M/NaCl 0.2 M is shown in Figure 4. The observed spectrum, (a), was subtracted by the monomer and tetramer bands, giving the spectrum of new aggregate, (b). The spectrum (b) consists mainly of a red-shifted peak at  $15,600 \text{ cm}^{-1}$  and a blue shifted at  $21,200 \text{ cm}^{-1}$ . These bands are separated by an equal wave number,  $2800 \text{ cm}^{-1}$ , from the dimer peak and the full widths at half maximum of both two peaks are approximately same as  $1000 \text{ cm}^{-1}$ . In general, the band of the red-shifted J-aggregate is known to exhibit an intense narrow fluorescence, while the blue shifted H-aggregate shows almost no fluorescence. However, for the new aggregate of DCI, no fluorescence has been detected either from the  $15,600 \text{ cm}^{-1}$  and  $21,200 \text{ cm}^{-1}$  excitation. According to the 1-dimensional exciton theory, the excited state of the chro-

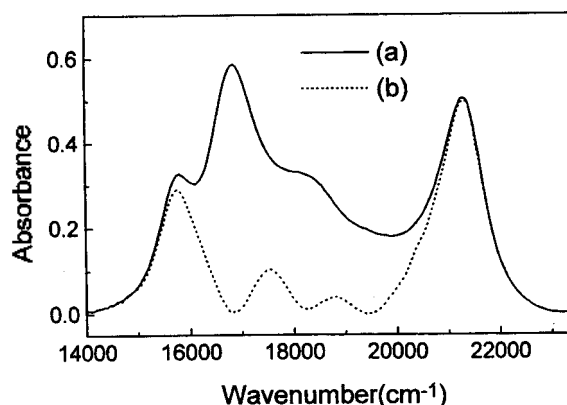


**Figure 4.** The observed absorption spectrum of  $10^{-3}$  M DCI/0.2 M NaCl in aqueous solution at room temperature is shown as (a). The spectrum of a new aggregate (b) is obtained by subtracting the monomer band and the trimer or tetramer band from the observed spectrum (a).

mophore will be split into two upon aggregation. In the aggregates having intermediate geometries between the parallel and head-to-tail orientations, the transitions to both of two state will be allowed to yield the blue and red sides of the absorption peak of the constituent chromophore. Therefore, we suggest that the new aggregate is formed by the aggregation of dimers and this aggregate would be in a intermediate geometry between the parallel and head-to-tail orientations.

In summary, the aggregations of 1,1'-diethyl-2,2'-carbocyanine iodide (DCI) and 1,1'-diethyl-2,2'-dicarbocyanine iodide (DDI) in aq were investigated by the steady-state absorption spectroscopy. The equilibrium constants for DCI and DDI are found to be  $(9.8 \pm 0.5) \times 10^4$  and  $(1.6 \pm 0.5) \times 10^5 \text{ M}^{-1}$ , respectively, at 293 K. The enthalpy changes for the dimerization of DCI and DDI are measured to be  $-6.7 \pm 0.7$  and  $-7.7 \pm 0.8 \text{ kcal/mol}$ , respectively. Assuming that the higher aggregate is the tetramer, the equilibrium constant for DCI tetramer formation is measured to be  $(5.2 \pm 0.3) \times 10^4$  at 293 K. With the same assumption in DDI solution, the equilibrium constant at 293 K and enthalpy change for DDI tetramer formation are  $(6.0 \pm 0.5) \times 10^4$  and  $-9.8 \pm 1.0 \text{ kcal/mol}$ , respectively. As the length of polymethine chain and the number of monomer in aggregate are increased, the aggregation is enhanced, showing that the dispersion force of DCI and DDI molecules is important in the aggregation. Almost zero entropy change in DCI/water dimerization indicates the participation of hydrophobic force. Temperature dependence of DCI absorption bandwidth in ethanol solution provides the evidence for no strong interaction between DCI and solvent molecules. We suggest that the aggregation of DCI can be driven by hydrophobic force. For the first time, DCI in aqueous solution is found to form the aggregate which has both J- and H- bands, showing little fluorescence activity.

**Acknowledgment.** This work has been supported by Korea Science and Engineering Foundation (941-0300-0432-2).

## References

1. (a) Feher, G.; Okamura, M. Y. In *The photosynthetic*

- bacteria*; Clayton, R. K.; Siström, W. F., Ed.; Plenum Press: New York, U. S. A. 1978; p 349. (b) Gilman, P. B. *Photo. Sci. Eng.* **1978**, *18*, 418. (c) Wang, Y. *Chem. Phys. Lett.* **1986**, *126*, 209. (d) Liang, Y.; Ponte Goncalves, A. M.; Negus, D. K. *J. Phys. Chem.* **1983**, *87*, 1. (e) Liang, Y.; Ponte Goncalves, A. M. *J. Phys. Chem.* **1985**, *89*, 3290. (f) Anfinrud, P. A.; Causgrove, T. P.; Struve, W. S. *J. Phys. Chem.* **1986**, *90*, 5887. (g) Anfinrud, P. A.; Crackel, R. L.; Struve, W. S. *J. Phys. Chem.* **1984**, *88*, 5873. (h) Crackel, R. L.; Struve, W. S. *Chem. Phys. Lett.* **1985**, *120*, 473.
- Arvan, Kh. L.; Zaitseva, N. E. *Opt. Spectrosc.* **1961**, *10*, 137.
  - (a) Valdes-Aguilera, O.; Neckers, D. C. *J. Phys. Chem.* **1988**, *92*, 4286. (b) Valdes-Aguilera, O.; Neckers, D. C. *Acc. Chem. Res.* **1989**, *22*, 171.
  - Sielcken, O. E.; van Tillborg, M.; Roks, M. F. M.; Hendriks, R.; Drenth, W.; Nolte, R. J. M. *J. Am. Chem. Soc.* **1987**, *109*, 4261.
  - West, W.; Pearce, S. *J. Phys. Chem.* **1965**, *69*, 1894.
  - (a) McRae, E. G.; Kasha, M. *J. Chem. Phys.* **1958**, *28*, 721. (b) McRae, E. G.; Kasha, M. In *Physical Processes in Radiation Biology*; Augenstein, L.; Rosenberg, B.; Mason, S. F., Ed.; Academic Press: New York, U. S. A. 1963.
  - Maeda, M. *Laser Dyes*; Academic Press: Tokyo, 1984.
  - Chen, S.-Y.; Horng, M.-L.; Quitevis, E. L. *J. Phys. Chem.* **1989**, *93*, 3683.
  - Emerson, E. S.; Conlin, M. A.; Rosenoff, A. E.; Norland, K. S.; Rodriguez, H.; Chin, D.; Bird, G. R. *J. Phys. Chem.* **1967**, *71*, 2396.
  - Graves, R. E.; Rose, P. I. *J. Phys. Chem.* **1975**, *79*, 746.
  - Kopainsky, B.; Hallermeier, J. K.; Kaiser, W. *Chem. Phys. Lett.* **1981**, *83*, 498.
  - Lax, M. *J. Chem. Phys.* **1952**, *20*, 1752.
  - Yu, J.; Berg, M. *J. Chem. Phys.* **1992**, *96*, 8741.
  - (a) Spano, F. C.; Mukamel, S. *Phys. Rev.* **1989**, *40*, 5783. (b) Carpenter, M. A.; Willand, C. S.; Penner, T. L.; Willwams, D. J.; Mukamel, S. *J. Phys. Chem.* **1992**, *96*, 2801. (c) Sasaki, F.; Kobayashi, S. *Appl. Phys. Lett.* **1993**, *63*, 2887.

## A New Model for the Reduced Form of Purple Acid Phosphatase: Structure and Properties of $[\text{Fe}_2\text{BPLMP}(\text{OAc})_2](\text{BPh}_4)_2$

Seon Hwa Yim, Ho Jin Lee, Kang-Bong Lee<sup>†</sup>,  
Seong Ju Kang<sup>†</sup>, Nam Hwi Hur<sup>‡</sup>, and Ho G. Jang<sup>\*</sup>

Contribution from the Department of Chemistry, Korea University, Seoul 136-701, Korea

<sup>†</sup>Advanced Analysis Center, KJIST, Seoul 136-130, Korea

<sup>‡</sup>Department of Chemical Education, Korea National University of Education, Chungbuk 363-791, Korea

<sup>\*</sup>Korea Research Institute of Standards and Science, Taejeon 305-600, Korea

Received February 12, 1998

$[\text{Fe}^{\text{II}}\text{Fe}^{\text{III}}\text{BPLMP}(\text{OAc})_2](\text{BPh}_4)_2$  (**1**), a new model for the reduced form of the purple acid phosphatases, has been synthesized by using a dinucleating ligand, 2,6-bis(((2-pyridylmethyl)(6-methyl-2-pyridylmethyl)amino)methyl)-4-methylphenol (HBPLMP). Complex **1** has been characterized by X-ray diffraction method as having ( $\mu$ -phenoxo)bis(acetato)diiron core. Complex **1** was crystallized in the monoclinic space group C2/c with the following cell parameters:  $a=41.620(6)$  Å,  $b=14.020(3)$  Å,  $c=27.007(4)$  Å,  $\beta=90.60(2)^\circ$ , and  $Z=8$ . The iron centers in the complex **1** are ordered as indicated by the difference in the Fe-O bond lengths which match well with typical  $\text{Fe}^{\text{III}}\text{-O}$  and  $\text{Fe}^{\text{II}}\text{-O}$  bond lengths. Complex **1** has been studied by electronic spectral, NMR, EPR, SQUID, and electrochemical methods. Complex **1** exhibits strong bands at 592 nm, 1380 nm in  $\text{CH}_3\text{CN}$  ( $\epsilon=1.0\times 10^3$ ,  $3.0\times 10^2$ ). These are assigned to phenolate-to- $\text{Fe}^{\text{III}}$  and intervalence charge-transfer transitions, respectively. Its NMR spectrum exhibits sharp isotropically shifted resonances, which number half of those expected for a valence-trapped species, indicating that electron transfer between  $\text{Fe}^{\text{II}}$  and  $\text{Fe}^{\text{III}}$  centers is faster than NMR time scale. This complex undergoes quasireversible one-electron redox processes. The  $\text{Fe}^{\text{III}}/\text{Fe}^{\text{II}}\text{Fe}^{\text{III}}$  and  $\text{Fe}^{\text{II}}\text{Fe}^{\text{III}}/\text{Fe}^{\text{II}}_2$  redox couples are at 0.655 and  $-0.085$  V vs SCE, respectively. It has  $K_{\text{comp}}=3.3\times 10^{12}$  representing that BPLMP/bis(acetate) ligand combination stabilizes a mixed-valence  $\text{Fe}^{\text{II}}\text{Fe}^{\text{III}}$  complex in the air. Complex **1** exhibits a broad EPR signal centered near  $g=1.55$  which is a characteristic feature of the antiferromagnetically coupled high-spin  $\text{Fe}^{\text{II}}\text{Fe}^{\text{III}}$  system ( $S_{\text{total}}=1/2$ ). This is consistent with the magnetic susceptibility study showing the weak antiferromagnetic coupling ( $J=-4.6$  cm<sup>-1</sup>,  $H=-2JS_1S_2$ ) between  $\text{Fe}^{\text{II}}$  and  $\text{Fe}^{\text{III}}$  center.

### Introduction

The purple acid phosphatases (PAP) constitute to a novel

class of non-heme metalloenzymes which catalyze the hydrolysis of certain phosphate esters under weak acidic condition.<sup>1</sup> Although they have been isolated from a variety of